NASA TECHNICAL MEMORANDUM

NASA TM X-62,099

NASA TM X-62,099

DIATOMIC GASDYNAMIC LASERS

Robert L. McKenzie

Ames Research Center
Moffett Field, Calif. 94035

December 1971

31 p

DIATOMIC GASDYNAMIC LASERS

Robert L. McKenzie
Ames Research Center, NASA
Moffett Field, California 94035

ABSTRACT

Predictions from a numerical model of the vibrational relaxation of anharmonic diatomic oscillators in supersonic expansions are used to show the extent to which the small anharmonicity of gases like CO can cause significant overpopulations of upper vibrational states. When mixtures of CO and N_2 are considered, radiative gain on many of the vibration-rotation transitions of CO is predicted. Experiments are described that qualitatively verify the predictions by demonstrating laser oscillation in CO-N_2 expansions. The resulting CO-N_2 gasdynamic laser displays performance characteristics that equal or exceed those of similar CO_2 lasers.

I. INTRODUCTION

Gasdynamic lasers have become well known as sources of extremely high laser power;[1] but until recently, CO_2 has been the only lasing constituent used in thermally excited high-power devices. Analytical models of the coupled nonequilibrium kinetic and fluid-dynamic processes in CO_2 systems have been successful when each CO_2 vibrational mode is treated as a separate harmonic oscillator.[2] The vibrational energy in each mode may then be assumed to be

distributed according to a Boltzmann population of vibrational states[3] and is commonly described by a spatially-dependent vibrational temperature that varies along the flow axis. However, this simplified harmonic oscillator model provides an accurate description of the nonequilibrium radiative properties of the expansion only when the lowest vibrational states are of interest, such as in the case with CO_2.[4] The application of a harmonic oscillator model to the relaxation of diatomic molecules leads to the conclusion that, within the single vibrational mode of a diatomic oscillator, a Boltzmann distribution also prevails and no population inversion will be induced by purely gasdynamic means.

Treaner, et al.[5] recently showed that the small decrease in spacing between anharmonic vibrational energy states with increasing quantum number introduces a new aspect to the vibrational relaxation process. In some circumstances, the small anharmonicity can cause upper level nonequilibrium populations to deviate from a Boltzmann distribution; particularly in a thermodynamic environment where the exchange of vibrational energy between oscillators is a dominant energy transfer mechanism. The exchange of vibrational energy between oscillators occurs at a rate that depends, in part, on the vibrational energy spacing of the states involved; so that in the case of rapidly expanding flows, those rate differences can result in an overpopulation of the upper states. Specifically, for flows originating at equilibrium temperatures comparable to the characteristic vibrational temperature of the oscillator and rapidly expanding to kinetic and rotational temperatures that are low relative to the characteristic vibrational temperature, population inversions between the combined

vibration-rotation levels of adjacent vibrational states may be induced. These inversions then provide the physical basis on which a diatomic gasdynamic laser may be operated.

In the following sections the above principles are demonstrated by first analytically studying the vibrational relaxation of anharmonic oscillator mixtures in supersonic expansions. Those studies rely on numerical solutions of the rate equations for the net production of oscillators in each vibrational quantum level considered. The calculations applied to CO admixtures illustrate the influence of vibrational exchange collisions on the nonequilibrium population distributions and radiative properties of CO. They also help define the proper gasdynamic conditions for a diatomic gasdynamic laser. The results of some laser experiments designed to verify the theoretical concepts are then described and the performance capabilities of a CO gasdynamic laser are indicated.

II. VIBRATIONAL RELAXATION OF ANHARMONIC OSCILLATORS IN EXPANDING FLOWS

In their studies of the relaxation of anharmonically spaced vibrational quantum states, Treanor et al.[5] wrote the rate equations for the population of each state. They included the usual terms accounting for collisional exchange of vibrational energy with the translational energy of the incident particle (V-T collisions), plus additional terms accounting for the exchange of vibrational energy between colliding oscillators (V-V collisions). They showed that in circumstances where the latter V-V terms dominate, the solution does not

require Boltzmann population distributions but, to zeroth order, has the more general form

$$N_j^V = N_j^o \exp(\alpha V - E_j^V/kT) \tag{1}$$

Here, N_j^V is the number density of oscillators of species j in vibrational quantum state, V, E_j^V is the energy of that state above the ground state, T is the translational temperature, and α is an additional time-dependent parameter related to the effective "vibrational temperature," U_{10}, of the first vibrational quantum state of species j by

$$\alpha = \frac{E_j^1}{kU_{10}}\left(\frac{U_{10}}{T} - 1\right) \tag{2}$$

The effects of oscillator anharmonicity may be injected by assuming a Morse internuclear potential, giving the oscillator energy of quantum state V above the ground state described by

$$E_j^V = k\theta_j V\{1 - \epsilon_j(V + 1)\} \tag{3}$$

where θ_j is the characteristic vibrational constant of species j, and ϵ_j is a small anharmonic coefficient ($\epsilon_j \ll \theta_j$). In a thermodynamic process where the kinetic temperature of the gas is reduced at a rapid rate compared to the mean vibrational relaxation time, U_{10} will lag the kinetic temperature and, from Eq. (2), α takes on growing positive values that approach $\alpha \approx \theta_j/T$. The product αV in Eq. (1) then nullifies the large linear terms in E_j^V leaving non-Boltzmann overpopulations of the upper states predicted by Eq. (1) that are determined mainly by the magnitude of the small anharmonic coefficient, ϵ_j, in Eq. (3).

Treanor's zeroth-order solution for α independent of quantum number applies well to the lower vibrational quantum states. At higher levels, however, V-T exchanges become dominate causing α to decrease with increasing quantum number in more exact calculations. To accurately study the process including higher quantum levels, a numerical code was constructed that solves the rate equations for an arbitrary spacing of oscillator energy states, number of species, and number of quantum levels. The formulation of the rate equations, numerical integration method, energy level truncation schemes, and solution characteristics are described in detail elsewhere.[6] The calculations contain no significant approximations, such as a first-moment approximation,[7] but rely on an implicit finite-difference scheme[8] for the numerical integration along an arbitrary one-dimensional flow axis. Similar calculations using a time-dependent integration method have recently been reported by Center and Caldonia.[9] The principle uncertainty in the calculations reported here and those of others[7,9] arises from the present uncertainty in collisional transition probabilities. However, Ref. 6 shows that the range of probability uncertainly does not affect the main qualitative features of the numerical solutions.

A sample calculation is illustrated in Fig. 1 for a CO expansion where the anharmonic CO population distribution at expansion area ratio $A/A_* = 200$ is compared with a harmonic oscillator solution and a distribution based on Eq. (1) for the same conditions. The anharmonic upper levels are significantly overpopulated when compared to the results of a harmonic oscillator model and, at

larger area ratios, eventually become inverted. The distribution of the lowest levels is well described by the zeroth order approximation of Eq. (1) as Treanor et al.[5] predict.

The effects of multiple, vibrationally relaxing, species and their interactions make up the situation of greatest interest. When a second species with energy levels of slightly greater spacing than those of the first is added to a cooling process such as an expansion, the upper level populations of the first species may be enhanced by additional V-V energy transfer. Using CO as an example; the addition of N_2 is suitable because it has slower V-T relaxation rates than CO, allowing N_2 to serve as a reservoir of vibrational energy that may be efficiently and rapidly transferred to the vibrational states of CO. Nitrogen can therefore be used in the same role with CO as it has been used in pumping the asymmetric-stretch mode of CO_2 in all CO_2-N_2 lasers. The vibrational exchange between CO and N_2 does not depend on the anharmonicity of either species, although it can be strongly affected by anharmonicity. Teare et al.[10] derive an expression for the locally equilibrated V-V exchange between harmonic oscillators, in terms of vibrational temperatures, $T_V(j)$, that may be applied here to CO and N_2 in the form

$$T_V(CO) = \theta_{CO} \Big/ \left[\frac{\theta_{N_2}}{T_V(N_2)} - \frac{\theta_{N_2} - \theta_{CO}}{T} \right] \tag{4}$$

Equation (4) shows that when $T_V(N_2)$ is sufficiently large in the presence of low translational temperatures, the CO vibrational temperature can become large and is not limited by even the initial reservoir value. An example of this

vibrational pumping has been demonstrated experimentally[10] and is illustrated in Fig. 2 by some numerical examples for anharmonic CO and N_2. The effect of oscillator anharmonicity is to invalidate the accuracy of Eq. (4) for large area ratios where the V-V controlled processes begin to lag behind the expansion cooling rate and are no longer locally equilibrated (i.e., they begin to freeze). Figure 3 indicates the range of validity of Eq. (4) for these examples by comparing $T_V(CO)_{NUM}$, the numerically computed vibrational temperatures of anharmonic CO based on the relative population of the first and ground state levels, with $T_V(CO)_4$, computed from Eq. (4) using local values of T and $T_V(N_2)$ from the numerical solution. The net effect of N_2 on the population distributions of anharmonic CO is shown in Fig. 4, where a comparison is made with the previous 100 percent CO case. The 5 percent CO/95 percent N_2 mixture obtains a greater number of CO molecules in all levels above the fourth and displays a flatter distribution, both of which contribute to greater radiative gain for transitions among those levels.

From the preceding, one may conclude that, for expanding flows, the effects of anharmonic energy states on the vibrational relaxation process must be included if populations of any (except the lowest) vibrational levels are of interest. Also, the addition of a second near-resonant species with slightly larger energy level spacings and a longer V-T relaxation time can significantly enhance the overpopulation of upper vibrational states in the primary species. The latter effect leads to a similar enhancement of radiative gain, a feature discussed in detail in the next section.

III. INFRARED RADIATIVE GAIN IN DIATOMIC GAS EXPANSIONS

The formulation of radiative gain coefficients for Doppler broadened vibration-rotation transitions has been summarized by Patel[11] in connection with a CO electric-discharge-laser analysis. The molecular circumstances in gasdynamic lasers are slightly different, however, since they usually operate at higher pressures in the laser cavity, thereby requiring the inclusion of collision broadening effects. The formulation of radiative gain with both broadening mechanisms has been described in detail in Ref. 6. The results are combined here with the previous vibrational relaxation calculations to provide an analysis of the radiative properties in diatomic gasdynamic expansions.

Following Patel,[11] some qualitative features of the P-branch vibration-rotation gain coefficients with only Doppler broadening are first shown in Fig. 5 for a coefficient normalized by all of the multiplying molecular constants, which are independent of rotational quantum number, J, or rotational temperature, T_r. Note that the vibrational population ratio $X_j^V/X_j^{V-1} = 0.8$, used in Fig. 5, does not represent a net vibrational inversion; although as T_r decreases, positive gains appear and strengthen. In the calculations to follow, gain coefficients are presented only for the P-branch rotational transition of maximum gain from each vibrational level.

Predicted gain coefficients are shown in Fig. 6 for several expanding CO-N_2 mixtures. As expected, expansions containing N_2 yield considerably higher gains than those with CO alone. Since optical loss coefficients

(analogous to the gain coefficients) for a moderate size research device are typically near 10^{-3} cm^{-1}, the results of Fig. 6 indicate that pure CO expansions can be made to lase only in unusually low-loss cavities or at conditions significantly different from those assumed here.

A second aspect of the radiative properties from diatomic expansions is associated with the gain enhancement obtained by reducing rotational temperature, as Fig. 5 indicates. Since rotational equilibration requires only a few collisions, the rotational energy (temperature) of most expansions may be assumed to be in thermal equilibrium with the local translational temperature. Thus, to enhance gain, the local translational temperature at a given geometric location in an expansion should be lowered without reducing the vibrational energy per molecule provided in the reservoir. This may be done using strictly thermodynamic effects by adding large fractions of a monatomic gas to increase the effective isentropic exponent. Argon is particularly suitable for this purpose because, as a heavy collision partner, it also reduces the rate of vibrational energy loss to translation through V-T collisions. The enhancement of gain obtained by diluting a 5 percent CO/95 percent N_2 mixture with 80 percent Ar is shown in Fig. 7. At area ratios less than 300, an order-of-magnitude increase in the gain coefficient is predicted and maximum gain occurs on transitions from lower vibrational levels.

The preceding results suggested two kinds of gas-mixture examples to demonstrate the aspects of anharmonic CO expansions. First, N_2-rich, CO-N_2

mixtures should yield ample gain for laser oscillation and possibly have the greatest efficiency because all species contain vibrational energy available for conversion to laser power. Second, CO-N_2 mixtures heavily diluted with argon should display the effect of enhanced gain over the former by providing laser power at lower area ratios and on lower vibrational transitions. Examples of both kinds of gas mixtures were chosen for the experiments described in the following sections.

IV. EXPERIMENTAL ARRANGEMENT

Mixtures of CO in N_2 and Ar were heated and supersonically expanded in the shock-tunnel arrangement illustrated in Fig. 8. The facility is operated by filling the driven tube with a test gas to pressures near 1 atm. A shock wave is generated in the tube by rupturing a double-diaphragm arrangement separating it from a high-pressure (200 atm) helium driver. The incident wave reflects from the driven-tube end wall, leaving a stagnant volume of compressed and heated gas that acts as the nozzle reservoir and remains nearly undisturbed for several milliseconds. The compressed reservoir gas ruptures a thin copper diaphragm and exhausts into the evacuated nozzle and dump tank. Expansion waves and helium from the driver then arrive and destroy the steady reservoir conditions. The nozzle was an axisymmetric 10° (half-angle) cone with a replaceable sonic throat area, A_*. Mirror ports with their optical axis perpendicular to the flow axis, were located at downstream positions, X = 41, 86, and 137 cm from the throat position, corresponding to optical path lengths of 14, 30,

and 48 cm. An optical cavity could be provided in any one of the ports by installing two circular mirrors, each with a 4.4 cm diam aperture and an inside spherical surface of 10 m radius. Power was removed through one mirror, made from a germanium substrate and coated for 3 percent transmission over the spectral region between 5 and 6 μm. Transmissivity rose through 14 percent at 4.7 μm. The other mirror was Al-coated glass with a reflectivity greater than 98 percent.

Laser power was measured during the 2 ms period of quasisteady flow by monitoring the temporal profile of the intensity pulse and measuring its total energy.[12] The intensity pulse was monitored with a fast-response Ge:Au detector viewing a small attenuated fraction of the beam reflected from a CaF_2 beam splitter. The remaining transmitted laser power was absorbed by a calibrated calorimeter that had greater accuracy and sensitivity than the one used in earlier measurements.[13] The combined pulse shape and energy measurements provided absolute time-dependent power values with an experimental uncertainty of less than 5 percent, to power levels below 0.5 W. Since the mirrors had to be removed and cleaned after each run, the repeatability from run to run was noticably affected by mirror alignment and surface condition. In the data to follow, curves are therefore faired through the data representing maximum power, assuming those points to be less than or equal to the laser performance with the mirrors properly aligned.

Spectral measurements were made with a 75 cm, grating monochrometer set at a different central wavelength for each run. The laser beam illuminated a NaCl diffusing plate located ahead of the entrance slit to help fill the instrument optics. A 75 groove/mm grating, blazed at 8 μm, was used in second order with a 1 mm exit slit giving a measured band pass of 0.017 μm. The 5 μm spectral signals were detected by a Ge:Au detector with a uniform spectral response between 4.5 and 6 μm.

Since hydrogen-bearing impurities are believed to have a large effect on vibrational relaxation rates, particularly in CO expansions,[14] attention was given to the test gas purity. Matheson "ultrahigh" purity CO and Ar and "prepurified" N_2 were mixed, as received, in an evacuated and outgassed mixing tank several days prior to their use. The driven tube was also purged with N_2 and evacuated before loading. These procedures are not sufficient to achieve the slowest vibrational relaxation rates reported by von Rosenberg et al.,[14] but represent a practical limit for convenient gasdynamic laser operation. From von Rosenberg's data, the conditions of these experiments are assumed to yield CO vibrational relaxation rates between 5 and 100 times faster than the slowest possible and consequently have an adverse effect on radiative gain.

V. EXPERIMENTAL RESULTS AND DISCUSSION

In the present nozzle configuration, only a small fraction of the total flow passed through the optical path. To compensate for the resulting power waste, the measured laser power has been transformed into that of a more idealized

nozzle and optical arrangement where most of the flow contributes energy to the laser beam. The transformation is accomplished by defining an efficiency based on the measured laser power normalized by the fraction of reservoir enthalpy flux intersected by the internal beam; namely,

$$\text{Eff} = \frac{P_L A}{H_o \dot{m} LD} \tag{5}$$

In Eq. (5), P_L is the measured laser power, H_o is the reservoir specific enthalpy, $\dot{m}$ is the total mass-flow-rate through the nozzle, A is the nozzle cross-section at the optical station, and L and D are the optical path length and aperature diameter.

Several gas mixtures were investigated initially,[13] including pure CO. No laser power was detected from CO alone but when N_2 was added, in the proportion N_2:CO = 3:1, laser power was obtained for a wide range of gasdynamic conditions; although at very low power levels for area ratios $A/A_* < 1000$. This effect of adding N_2 substantiates the predicted influence of V-V energy pumping from N_2 to CO illustrated in Fig. 2 and the resulting gain enhancement shown in Fig. 6. The addition of the third component, Ar, caused significant increases in power from lower area ratios as Figs. 9 and 10 depict. These results demonstrate the influence of decreased rotational excitation in expansions with a larger isentropic exponent. Similar results with less amounts of Ar may be possible from more rapidly expanding flow geometries. The proportions of N_2 and CO were also varied using a fixed Ar concentration of 80 percent by volume.

In Ar-diluted mixtures, the continued addition of N_2 enhanced laser power only slightly until, as Fig. 9 shows, the remaining CO content became too small and laser power rapidly decreased. In the other extreme without N_2, the remaining argon-rich CO-Ar mixture had a sufficiently increased cooling rate to provide ample gain for lasing. This feature was first demonstrated by Watt[15] and appears in Fig. 9 for a 20 percent CO/80 percent Ar mixture. The ineffectiveness of N_2 addition in Ar-diluted mixtures indicates that, although N_2 enhances the development of radiative gain during the expansion upstream of the optical cavity, the several hundred collisions that occur between CO and N_2 molecules during the short period the flow passes through the optical cavity are not adequate to transfer any significant amount of N_2 vibrational energy to the expended CO laser states. These results are reasonable in view of the V-V probability magnitudes which are usually less than 10^{-2}. Similar behavior is observed in CO_2 gasdynamic lasers and is corrected by extending the cavity optics in the flow direction. For example, the efficiency [as defined by Eq. (5)] of a combustion powered 6 KW CO_2-N_2 gasdynamic laser device reported by Gerry[1] reached values near 0.13 percent with a 3 cm-square cavity viewing all of the flow. This case can be compared to the configuration of these CO experiments and suggest that the CO gasdynamic laser performance equals or exceeds that of a similar CO_2 device. However, when Gerry extended the CO_2 laser cavity 20 cm downstream, he obtained a three fold increase in total power or efficiency. The efficiencies reported here are therefore not representative of the maximum capabilities of a properly designed CO laser system.

Performance was also investigated for a range of area ratios, A/A_*, and throat diameters, d_*. The results, depicted in Fig. 10, show that laser power may be obtained at area ratios as low as 120. Such area ratios are still large in comparison to values between 10 and 50, commonly used in CO_2 gasdynamic lasers, but an associated feature favorable to the CO expansions is the much larger throat sizes allowable. The lowest area ratios indicated for each axial location, X, in Fig. 10 were obtained using a throat diameter, $d_* = 1.27$ cm. This may be compared to the CO_2 expansions that require throat dimensions less than 0.1 cm to maximize their laser performance.[1,12] Thus, many of the aerodynamic, cooling, and mechanical problems associated with the small throats of CO_2 devices will be less restrictive in a similar CO system.

The product of reservoir pressure and throat diameter, $P_o d_*$, has often been identified as a similarity parameter for nonequilibrium flows in nozzles with a given divergence angle.[16] Thus, verification that throat size can be further increased without loss of performance is shown by the data in Fig. 11 where its equivalent variable, P_o, has been increased. At pressures above 80 atm laser power increases nearly linearly with pressure to the limits of the apparatus. The constant slope described by the data corresponds to an efficiency of 0.17 percent or a specific laser power of 2.2 W per g/s of total mass flow. Laser power was obtained with reservoir pressures as low as 20 atm at $A/A_* = 1455$ and $d_* = 1.27$ cm in argon-rich mixtures.

The variation of laser power with reservoir temperature is shown in Fig. 12. As the scales of the figure imply, reservoir temperature is inferred from the incident shock speed measurements. The data indicate that maximum power or efficiency is obtained at temperatures close to those at which the CO_2 lasers perform best.[4,12]

Spectral measurements in addition to those reported previously[13] were made at an area ratio $A/A_* = 577$. In the absence of a rapid-scan spectrometer, separate shock-tube firings were required for each monochrometer setting and many shots were necessary to cover the entire multimode laser spectrum. Hence, only a few spectral settings were repeated. The repeated settings showed the spectral intensity to have extremely poor repeatability, possibly due to a laser frequency dependence on the mirror alignment. The relative magnitudes of the spectral data are therefore not a reliable indication of the spectral intensity distribution of the laser. Consequently, only the spectral location at which laser power was observed, their apparent transition and a course indication of the relative power at the transition are listed in Table I. The spectral measurements generally support the predictions of gain given here and in Ref. 6, in that, as the area ratio is increased, transitions from lower vibrational states appear or lase with greater power. Adding Ar is, in part, equivalent to increasing the area ratio because the rotational temperature is reduced in both cases. Hence, the spectral data understandably show that mixtures with Ar also lase with greatest power from lower vibrational levels than those without Ar.

Finally, both mixtures were observed to lase with greatest power near the transitions of predicted maximum gain. For comparison, examples of some gain predictions using the experimental conditions are shown in Fig. 13. The calculations incorporate very conservative V-T relaxation rates, increased by a factor of 100 over the values measured behind shock waves,[17] to account for the maximum reasonable effects of impurities.[14] The magnitudes of the V-T rates mostly affect the gain magnitude, however, and have no large influence on its distribution at these conditions. The V-V rates used are comparable with measurements[18] obtained at 300°K. However, rate calculations including long-range interactions[19] lead to the conclusion that all the V-V rates used here and by others[7,9] are very uncertain at lower temperatures. Finally, the comparison of small signal gain predictions and observed laser transitions is confused by the effects of gain saturation and induced cascading among vibrational levels during laser oscillation; so that these gain predictions can only be used as an indication of the most likely laser transitions but cannot be compared in detail with the laser spectral power distribution.

VI. CONCLUSIONS

Predictions from a numerical model of the vibrational relaxation of anharmonic diatomic oscillators in supersonic expansions have shown that the small anharmonicity of gases like CO can cause significant overpopulation of upper vibrational states when the vibration-vibration energy transfer is a dominate mechanism. The combined vibration-vibration energy exchange

between near-resonant oscillators of unlike species further enhances the overpopulation of one type at the expense of the other. When coupled with the infrared radiative properties of a permanent-dipole oscillator, the above features lead to predictions of radiative gain sufficient to drive laser oscillation.

Experiments using thermally-heated expansions of CO and N_2 were performed to test the foregoing theoretical results. The experimental results clearly verify the anharmonic effects on the nonequilibrium vibrational energy distribution by demonstrating the achievement of laser oscillation with significant power. For the conditions of the experiment, laser power and efficiency were enhanced when the vibrational species were diluted with argon. The resulting CO-N_2-Ar gasdynamic laser displayed performance characteristics that equal or exceed the performance of similar CO_2-N_2 gasdynamic lasers; even for the non-idealized optical cavity and nozzle geometry used in these experiments. Laser power has been obtained over a wide range of gasdynamic conditions and on many spectral lines in the wave length region from 4.78 to 5.4 μm. The requirements of a CO gasdynamic laser expansion have been shown to differ from those for a CO_2 system only in that it will require area ratios and throat dimensions typically 10 times greater than the CO_2 system. The thermal requirements of the reservoir are similar.

The CO gasdynamic laser characteristics described here depend, to a large part, on the nozzle and optical configurations of the experiment. In addition, the use of pure thermal excitation for high-power lasers does not provide the efficiency

obtained by recent chemically[20] or electrically[21,22] excited systems. The significant aspect of these experiments, therefore, is the demonstrated enhancement of radiative gain and energy-pumping to laser levels that may be obtained from a process dominated by anharmonic V-V exchange. The stimulation of these processes in conjunction with excitation schemes that more selectively excite upper vibrational states[20,21,22] should allow extension of the resulting high gain regions to larger volumes and enhance the restoration rates of expended laser levels.

VII. REFERENCES

1. E. T. Gerry, IEEE Spectrum 7, 51 (Nov. 1970).
2. J. D. Anderson, Phys. Fluids 13 1983 (1970).
3. E. W. Montroll and K. E. Shuler, J. Chem. Phys. 26, 454 (1957).
4. G. Lee and F. E. Gowen, Appl. Phys. Letters 18 237 (1971).
5. C. E. Treanor, J. W. Rich, and R. G. Rehm, J. Chem. Phys. 48 1798 (1968).
6. R. L. McKenzie, NASA TN D-7050 (1971).
7. K. N. C. Bray, J. Phys. B. (Proc. Phys. Soc.), Ser. 2, 1 705 (1968).
8. H. E. Bailey, Phys. Fluids 12 2292 (1969).
9. R. E. Center and G. E. Caledonia, Applied Optics 10 1795 (1971).
10. J. D. Teare, R. L. Taylor, and C. W. Von Rosenberg, Nature 225 240 (1970).
11. C. K. N. Patel, Phys. Rev. 141 71 (1966).
12. D. M. Kuehn and D. J. Monson, Appl. Phys. Letters 16 48 (1970).
13. R. L. McKenzie, Appl. Phys. Letters 17 462 (1970).
14. C. W. von Rosenberg, R. L. Taylor, and J. D. Teare, J. Chem. Phys. 48 5731 (1968).
15. W. S. Watt, Applied Phys. Let. 18 487 (1971).
16. J. L. Stollery and C. Park, J. of Fluid Mech. 19 113 (1964).
17. W. J. Hooker and R. C. Millikan, J. Chem. Phys. 38 214 (1963).
18. G. Hancock and I. W. M. Smith, Appl. Optics 10 1827 (1971).

19. R. D. Sharma and C. A. Brau, J. Chem. Phys. 50 924 (1969).

20. D. J. Spencer, H. Mirels, and T. A. Jacobs, Appl. Phys. Letters 16 384 (1970).

21. A. E. Hill, Appl. Phys. Letters 16 423 (1970).

22. J. W. Rich, H. M. Thompson, C. E. Treanor, and J. W. Daiber, Applied Phys. Let. 19 230 (1971).

Table I. Observed spectral locations.

Conditions[a]	Wavelength (μm)	Apparent ΔV	Transition Rot. Line[b]	Relative Intensity[c]
5%CO-15%N_2-80%Ar $A/A_* = 577$	4.847	3-2	P(7)	S
	4.899	4-3	P(6)	S
	4.963	5-4	P(6)	S
	5.028	6-5	P(9)	W
5%CO-15%N_2-80%Ar $A/A_* = 2730$	4.78	2-1		S
	4.84	3-2		S
	4.90	4-3		M
	4.96	5-4		M
	5.02	6-5		M
	5.07	7-6		W
	5.14	8-7		W
	5.26	9-8		W
25%CO-75%N_2 $A/A_* = 2730$	4.84	3-2		W
	4.90	4-3		W
	4.96	5-4		W
	5.047	6-5	P(8)	S
	5.10	7-6		M
	5.20	8-7		M
	5.26	9-8		W
	5.40	11-10		W

[a] The other experimental conditions were $T_o = 2100°K$, $P_o = 85$ atm, throat diameter = 1.27 cm.

[b] Where the spectrometer setting has been centered on selected rotational lines, the line of greatest intensity is listed. Weaker adjacent lines were also observed in most cases.

[c] Relative intensities are given as W-weak, M-moderate, S-strong.

FIGURE TITLES

Fig. 1. Population distributions at $A/A_* = 200$ for harmonic and anharmonic CO expanding in a two-dimensional supersonic nozzle with a 15° divergence half-angle and a 0.127-cm throat height. Reservoir conditions were $P_o = 100$ atm and $T_o = 2000°K$.

Fig. 2. Vibrational temperatures normalized by the reservoir temperature, T_o, in expansions of anharmonic CO-N_2 mixtures. The vibrational temperatures are determined from the relative populations of the first and ground vibrational energy state of each species. (Nozzle conditions are the same as for Fig. 1.)

Fig. 3. Comparison of the CO vibrational temperature for a harmonic oscillator model calculated from Eq. (4) and the anharmonic CO vibrational temperature of the first and ground state populations from numerical solutions. (Nozzle conditions are the same as Fig. 1.)

Fig. 4. The effect of N_2 on the population distributions of CO at $A/A_* = 200$. (Nozzle conditions are the same as for Fig. 1.)

Fig. 5. Normalized P-branch gain coefficients for Doppler-broadened vibration-rotation transitions from a partial ($X^V/X^{V-1} < 1$) vibrational inversion.

Fig. 6. CO gain coefficients at $A/A_* = 200$ in CO-N_2 expansions. (Nozzle conditions are the same as for Fig. 1.)

Fig. 7. The effect of Ar dilution on CO gain coefficients in CO-N_2-Ar expansions. V is the upper level vibrational quantum number. (Nozzle conditions are the same as in Fig. 1.)

Fig. 8. Shock tunnel and instrumentation arrangement.

Fig. 9. The effect of gas composition on laser efficiency. Test conditions were P_o = 85 atm, T_o = 2100°K, A/A_* = 577, d_* = 1.27 cm.

Fig. 10. The effect of area ratio and throat diameter on laser efficiency. Reservoir conditions were P_o = 85 atm, T_o = 2100°K.

Fig. 11. The effect of reservoir pressure on laser energy flux. Test conditions were T_o = 2100°K, A/A_* = 577, d_* = 1.27 cm.

Fig. 12. The effect of reservoir temperature on laser energy flux. Test conditions were 5%CO-15%N_2-80%Ar, P_o = 90 atm, A/A_* = 577, d_* = 1.27 cm.

Fig. 13. Gain predictions for the experimental conditions at P_o = 100 atm, T_o = 2100°K, d_* = 1.27 cm.

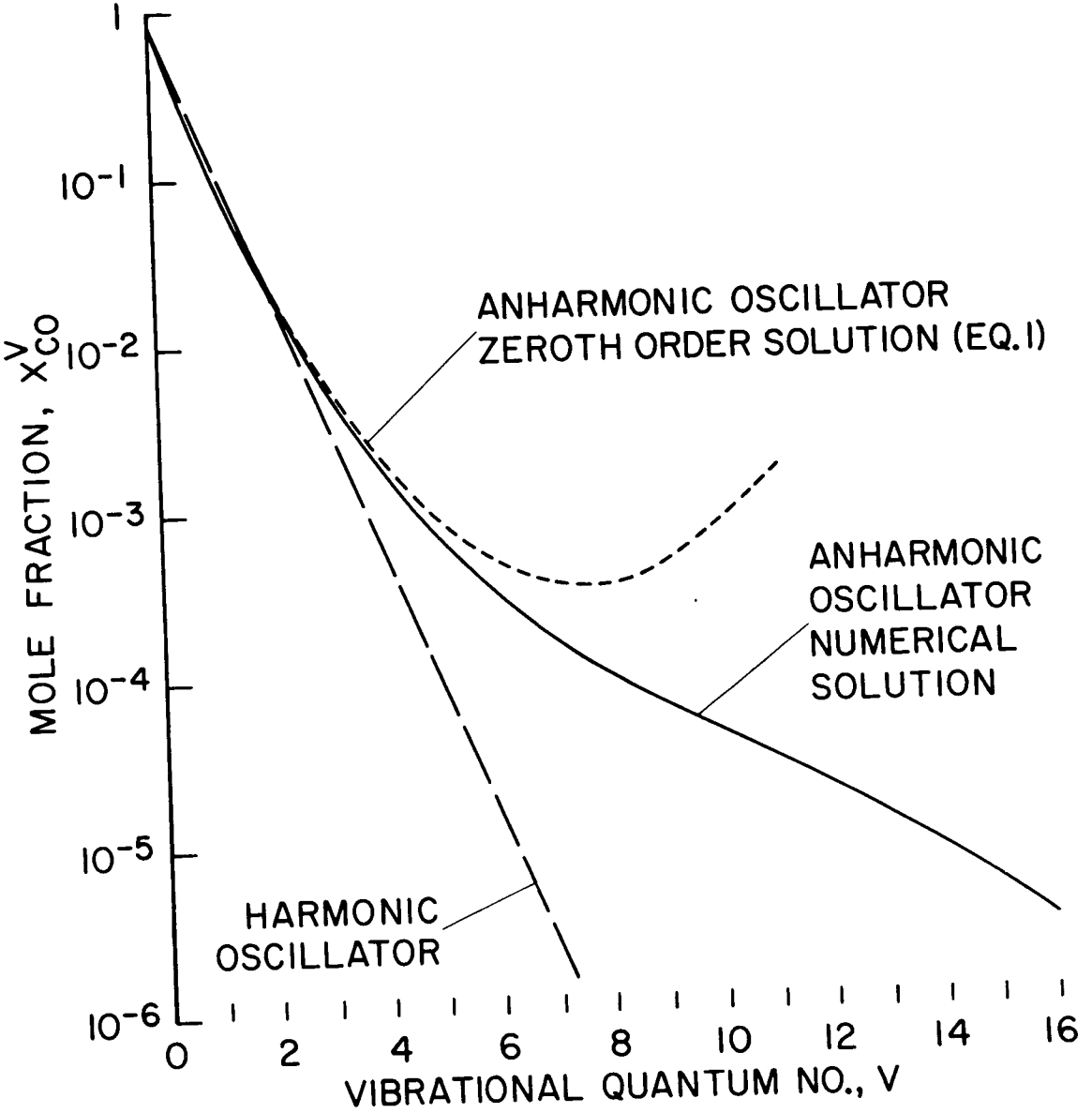
1
10-1
10-2
10-3
10-4
10-5
10-6
MOLE FRACTION, X_{CO}^{V}
ANHARMONIC OSCILLATOR
ZEROTH ORDER SOLUTION (EQ.1)
ANHARMONIC
OSCILLATOR
NUMERICAL
SOLUTION
HARMONIC
OSCILLATOR
0
2
4
6
8
10
12
14
16
VIBRATIONAL QUANTUM NO., V

Figure 1

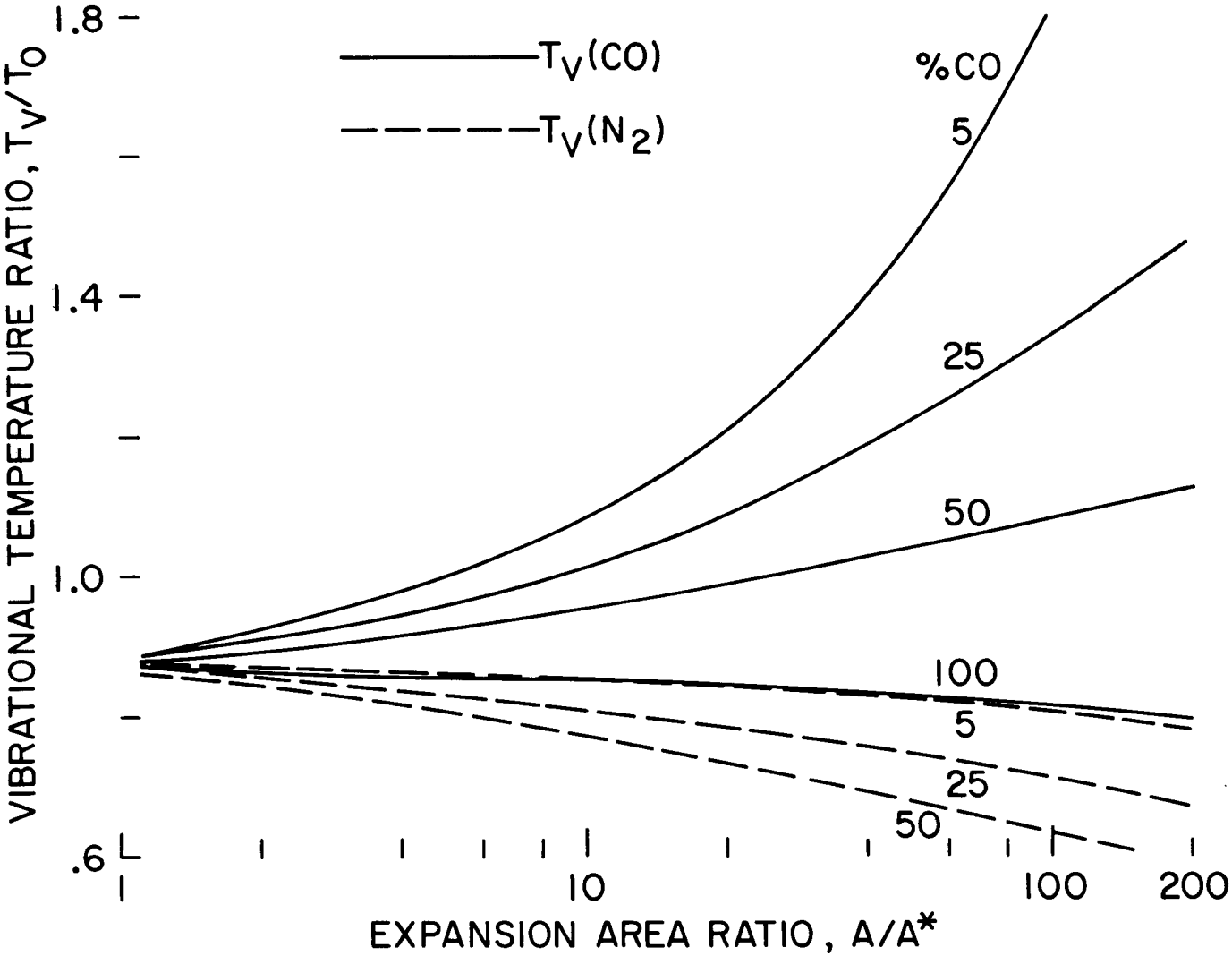
VIBRATIONAL TEMPERATURE RATIO, T_V/T_0
1.8
1.4
1.0
.6
$T_V(CO)$
$T_V(N_2)$
%CO
5
25
50
100
5
25
50
10
100
200
EXPANSION AREA RATIO, A/A*

Figure 2

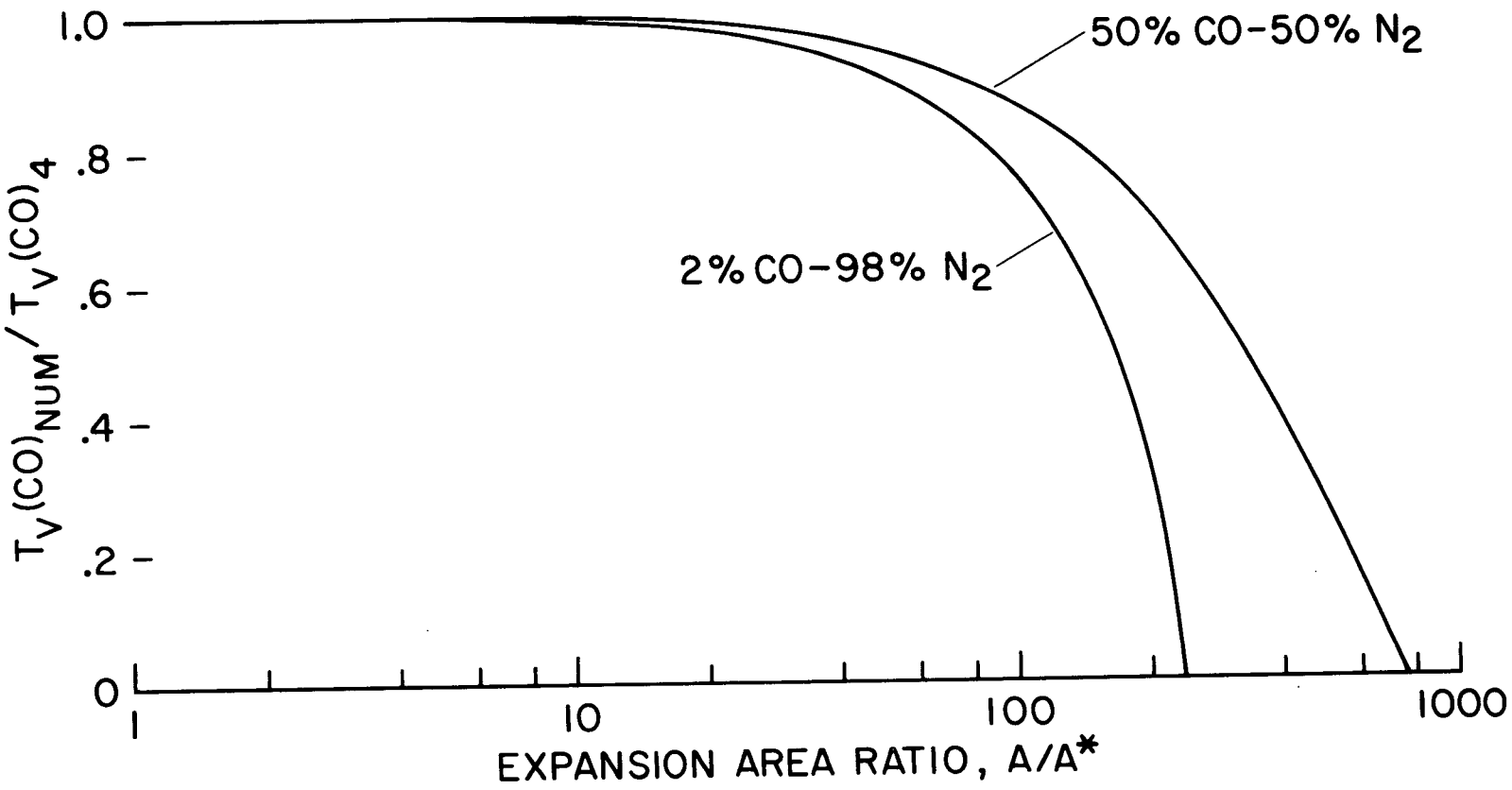
1.0
.8
.6
.4
.2
0
$T_{V(CO)_{NUM}} / T_{V(CO)_4}$
50% CO-50% N_2
2% CO-98% N_2
1
10
100
1000
EXPANSION AREA RATIO, A/A*

Figure 3

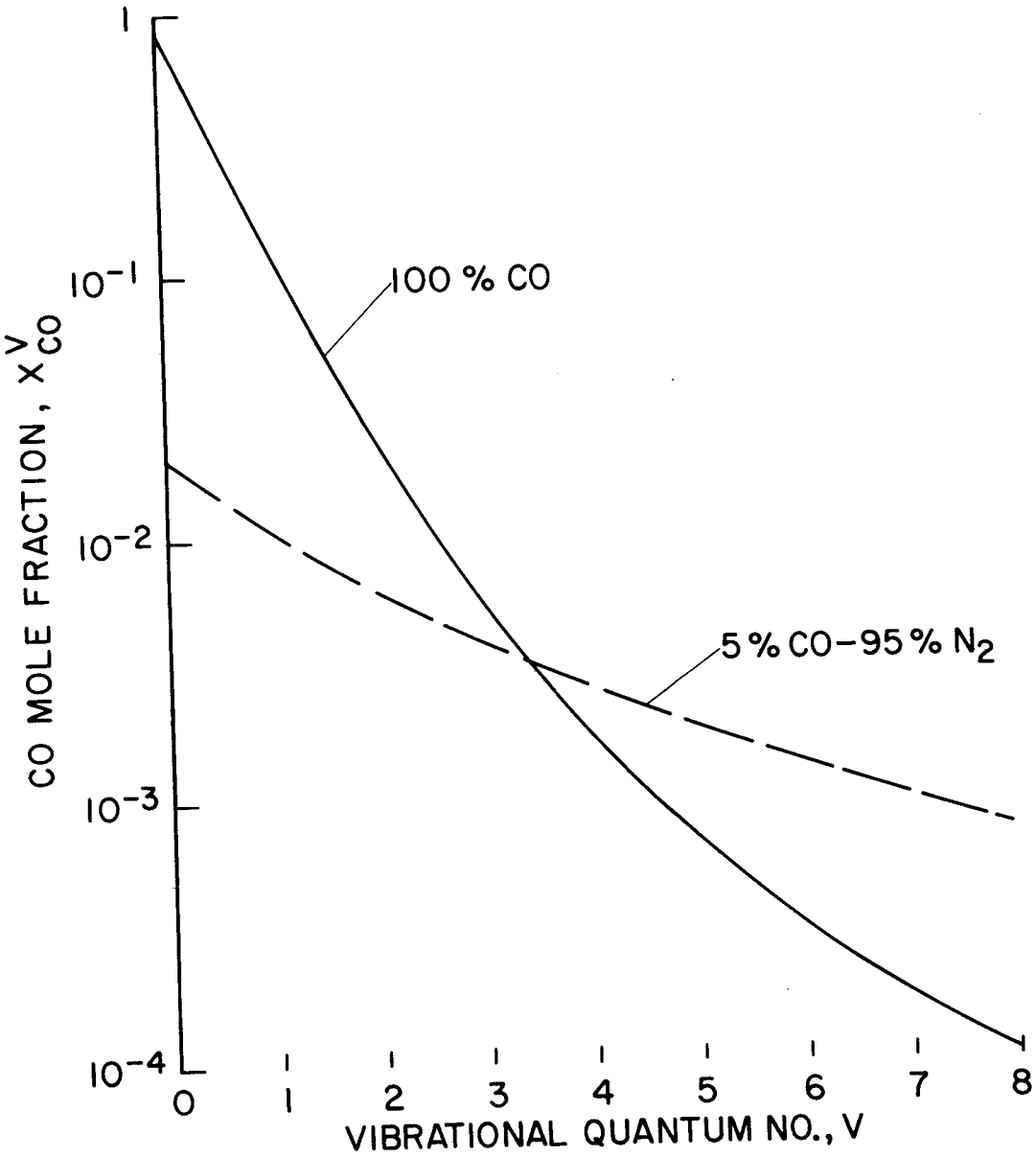
1
10^{-1}
10^{-2}
10^{-3}
10^{-4}
CO MOLE FRACTION, X_{CO}^{V}
100 % CO
5 % CO–95 % N_2
0
1
2
3
4
5
6
7
8
VIBRATIONAL QUANTUM NO., V

Figure 4

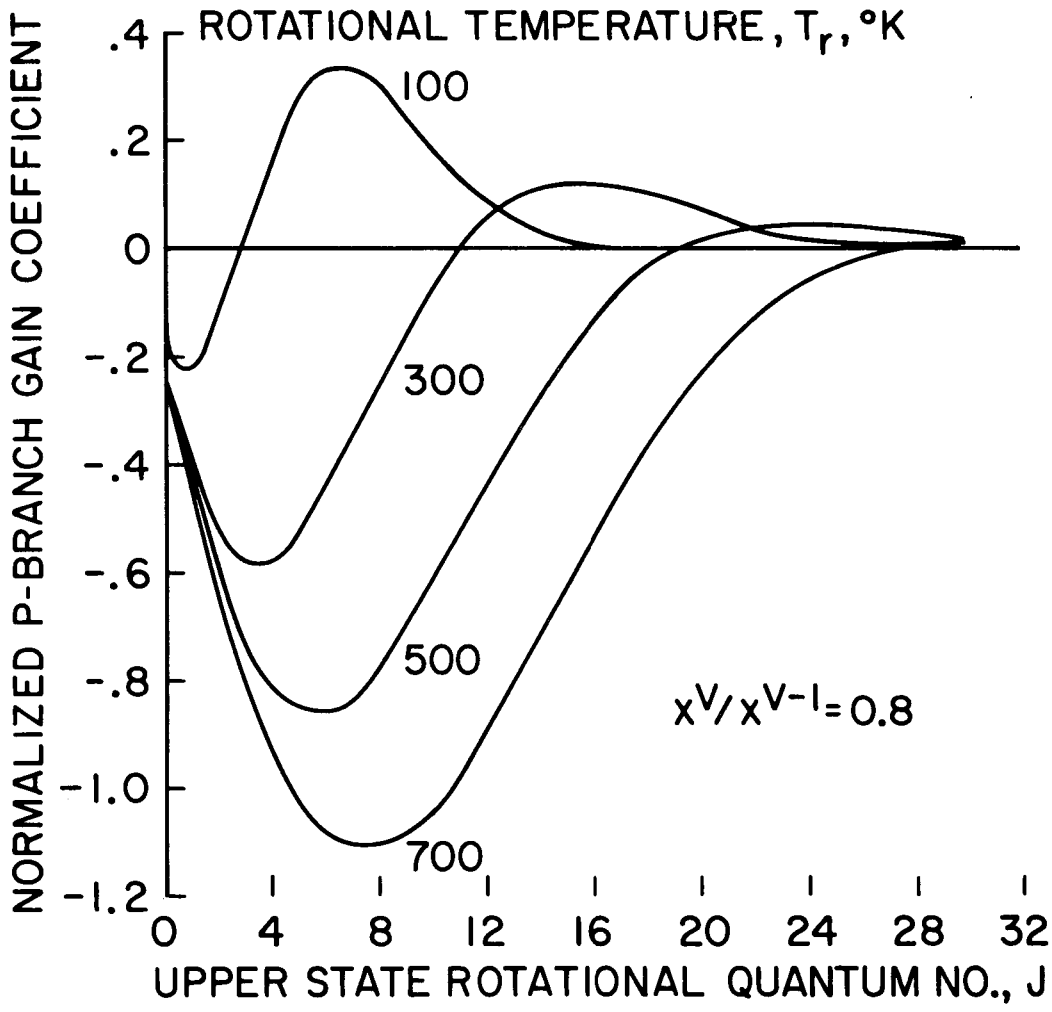
ROTATIONAL TEMPERATURE, T_r, °K
100
300
500
700
$x^V/x^{V-1}=0.8$
NORMALIZED P-BRANCH GAIN COEFFICIENT
.4
.2
0
-.2
-.4
-.6
-.8
-1.0
-1.2
0
4
8
12
16
20
24
28
32
UPPER STATE ROTATIONAL QUANTUM NO., J

Figure 5

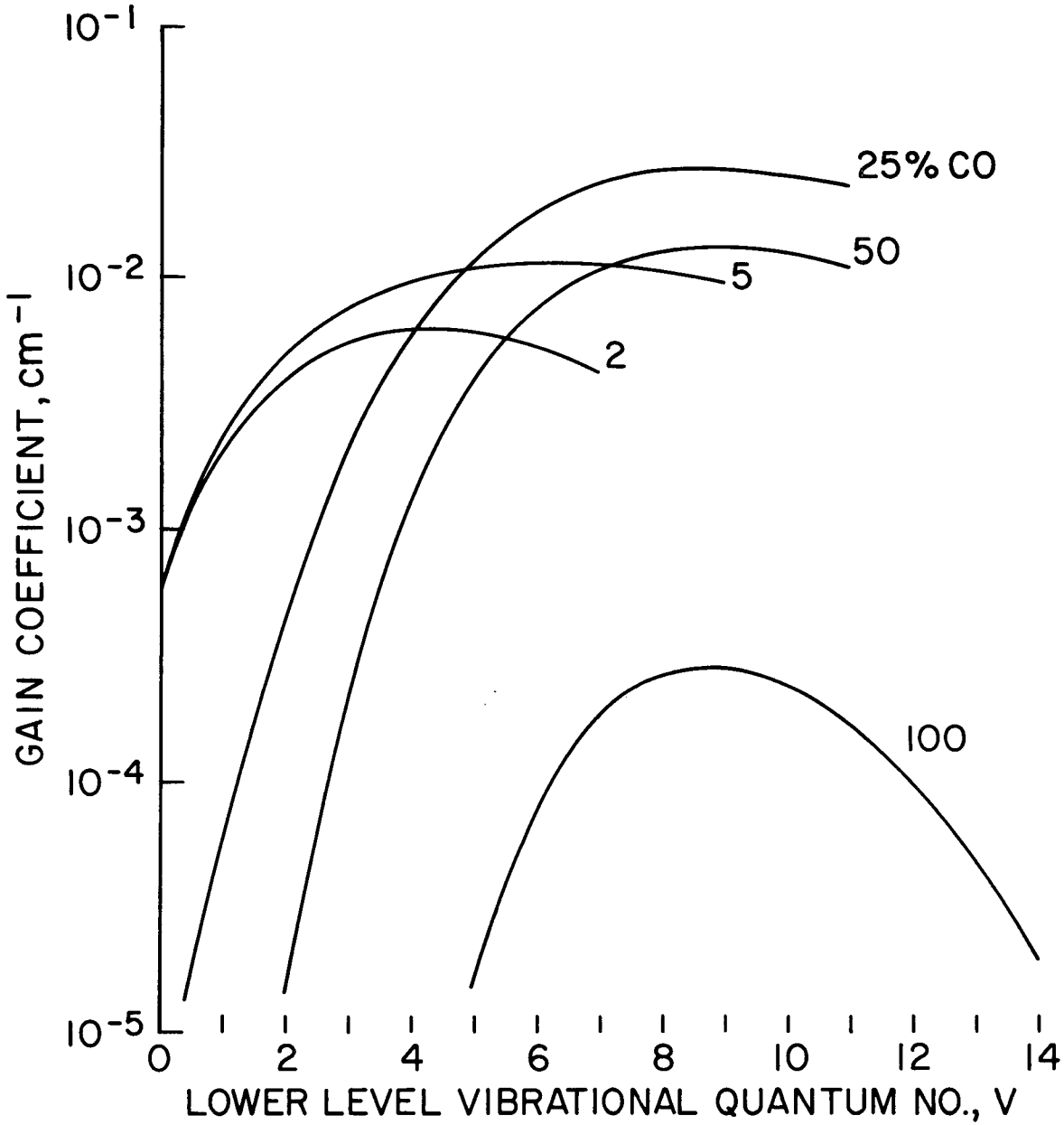
10^{-1}
10^{-2}
10^{-3}
10^{-4}
10^{-5}
GAIN COEFFICIENT, cm^{-1}
25% CO
50
5
2
100
0
2
4
6
8
10
12
14
LOWER LEVEL VIBRATIONAL QUANTUM NO., V

Figure 6

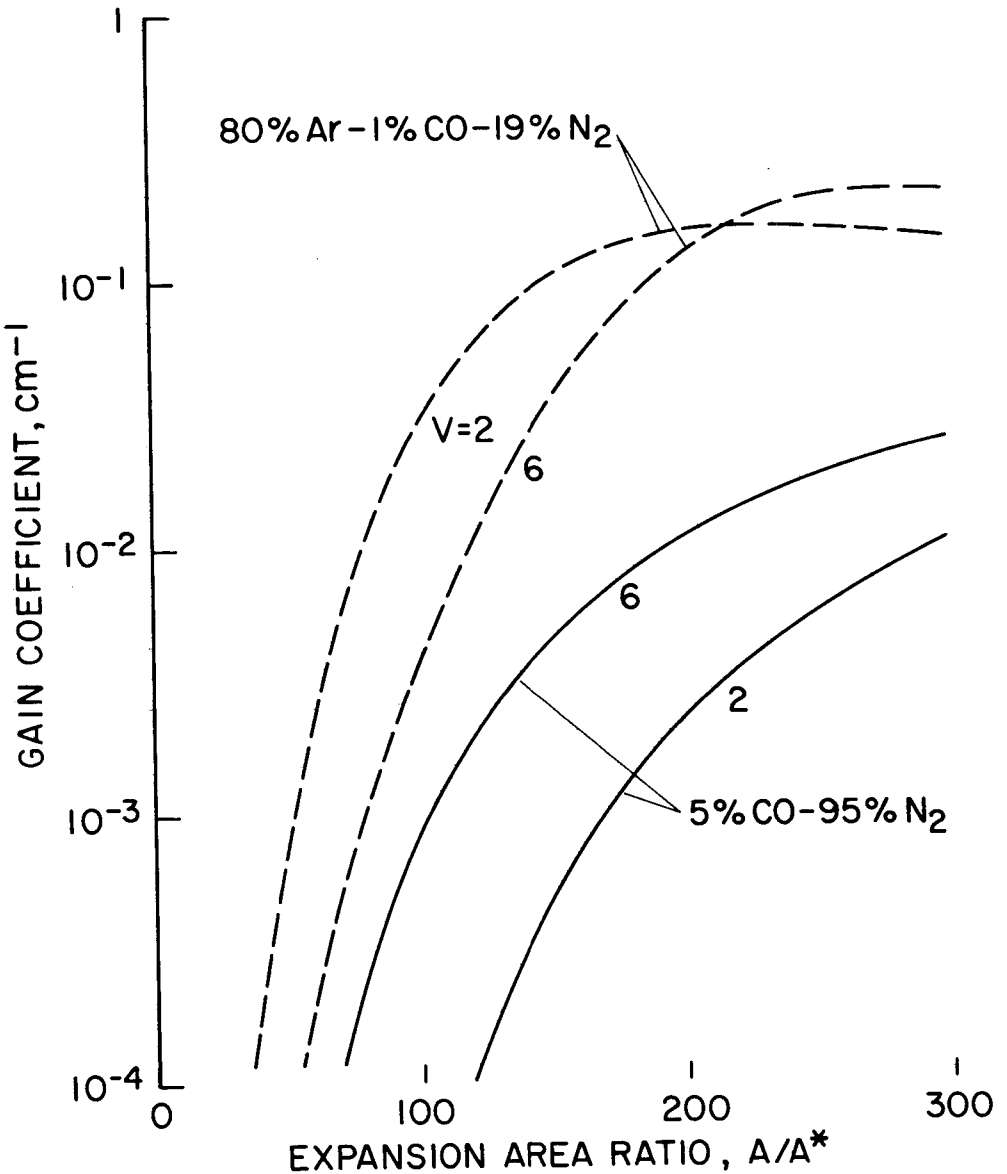
1
10^{-1}
10^{-2}
10^{-3}
10^{-4}
GAIN COEFFICIENT, cm^{-1}
80% Ar - 1% CO - 19% N_2
V=2
6
6
2
5% CO - 95% N_2
0
100
200
300
EXPANSION AREA RATIO, A/A*

Figure 7

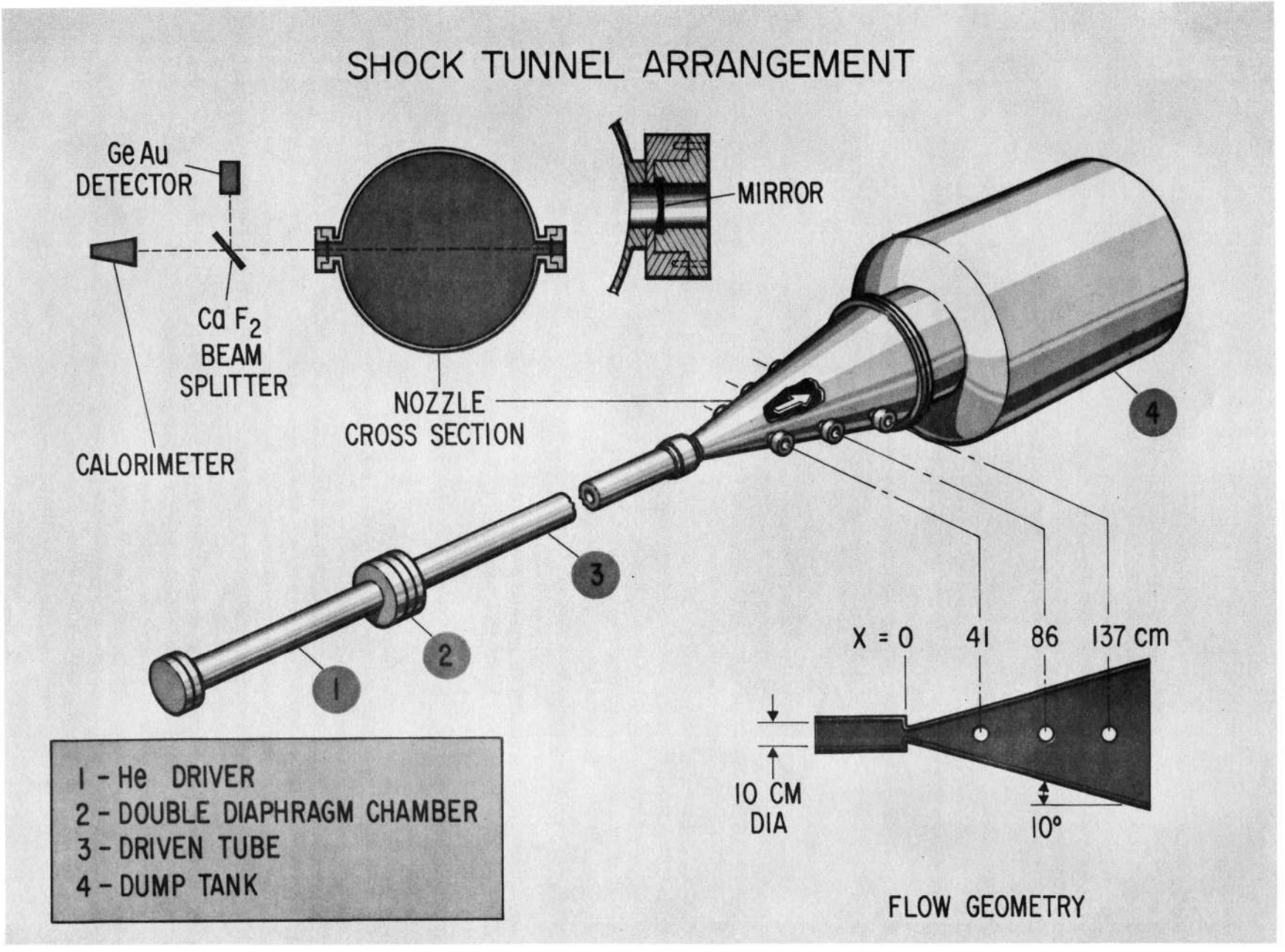
SHOCK TUNNEL ARRANGEMENT
Ge Au
DETECTOR
MIRROR
Ca F2
BEAM
SPLITTER
NOZZLE
CROSS SECTION
CALORIMETER
1 - He DRIVER
2 - DOUBLE DIAPHRAGM CHAMBER
3 - DRIVEN TUBE
4 - DUMP TANK
X = 0
41
86
137 cm
10 CM
DIA
10°
FLOW GEOMETRY

Figure 8.

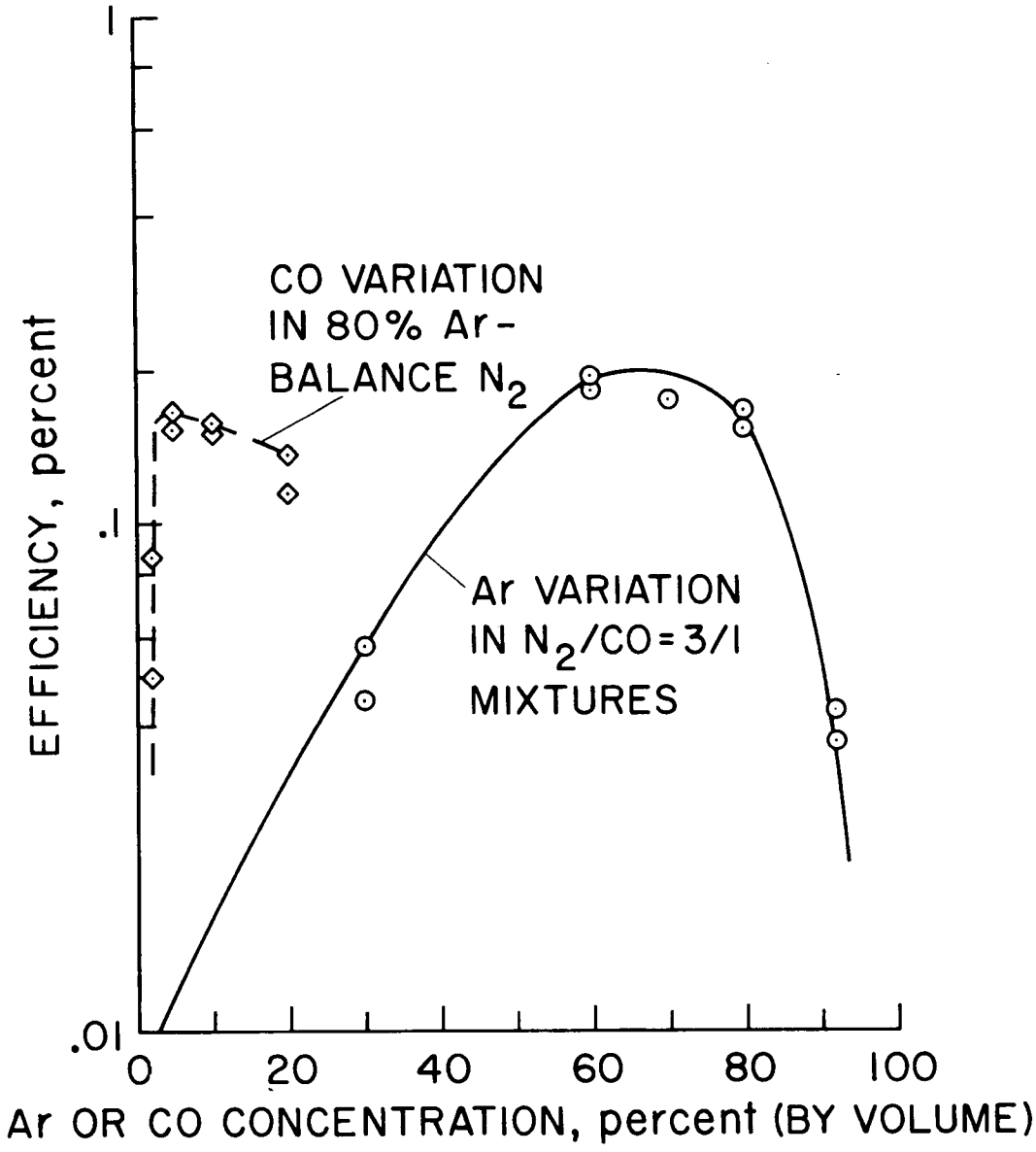
1
.1
.01
EFFICIENCY, percent
CO VARIATION
IN 80% Ar-
BALANCE N_2
Ar VARIATION
IN N_2/CO=3/1
MIXTURES
0
20
40
60
80
100
Ar OR CO CONCENTRATION, percent (BY VOLUME)

Figure 9

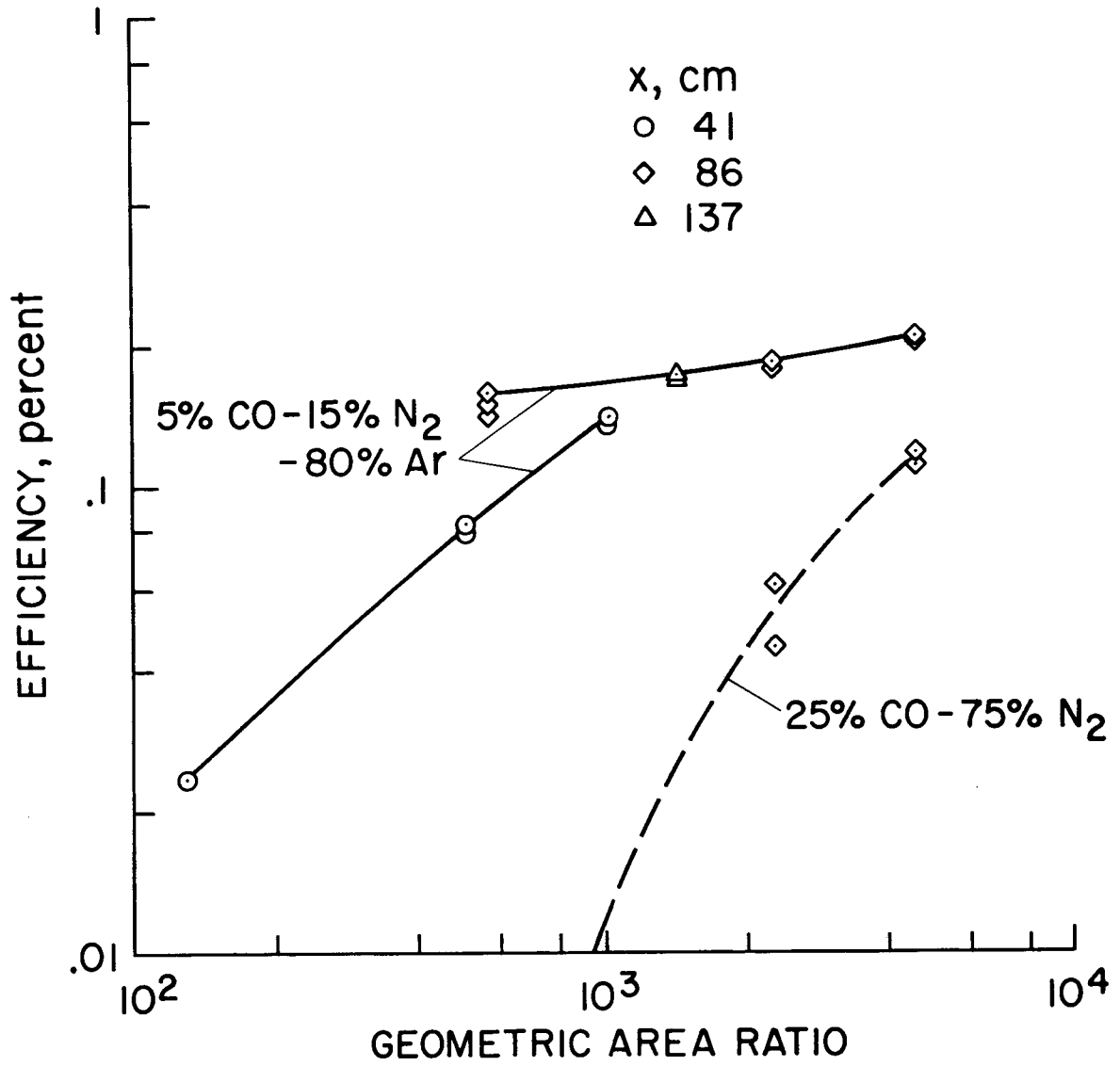
1
.1
.01
EFFICIENCY, percent
x, cm
41
86
137
5% CO-15% N2
-80% Ar
25% CO-75% N2
10^2
10^3
10^4
GEOMETRIC AREA RATIO

Figure 10

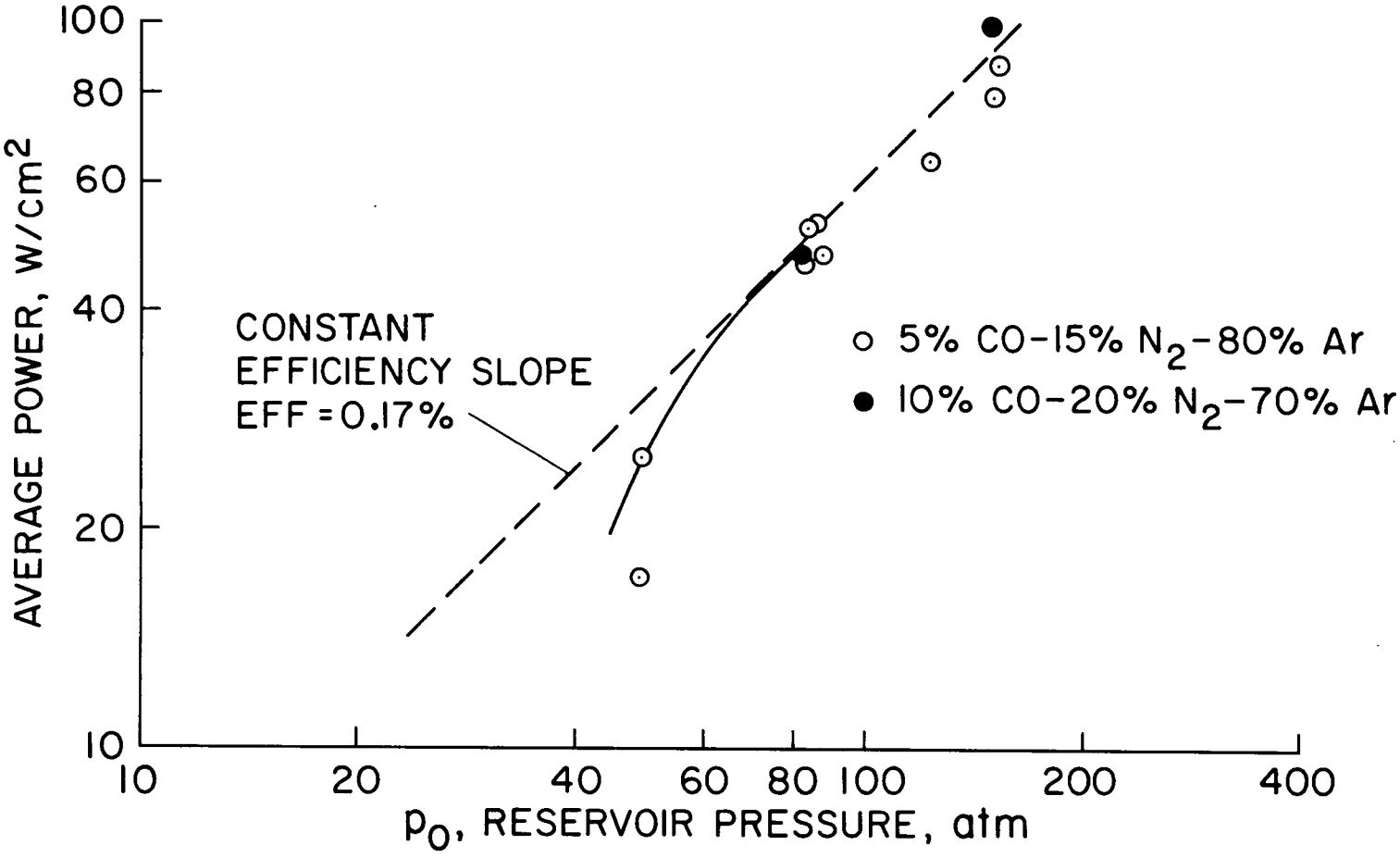
100
80
60
40
20
10
AVERAGE POWER, W/cm2
CONSTANT
EFFICIENCY SLOPE
EFF = 0.17%
5% CO-15% N2-80% Ar
10% CO-20% N2-70% Ar
10
20
40
60
80
100
200
400
p0, RESERVOIR PRESSURE, atm

Figure 11

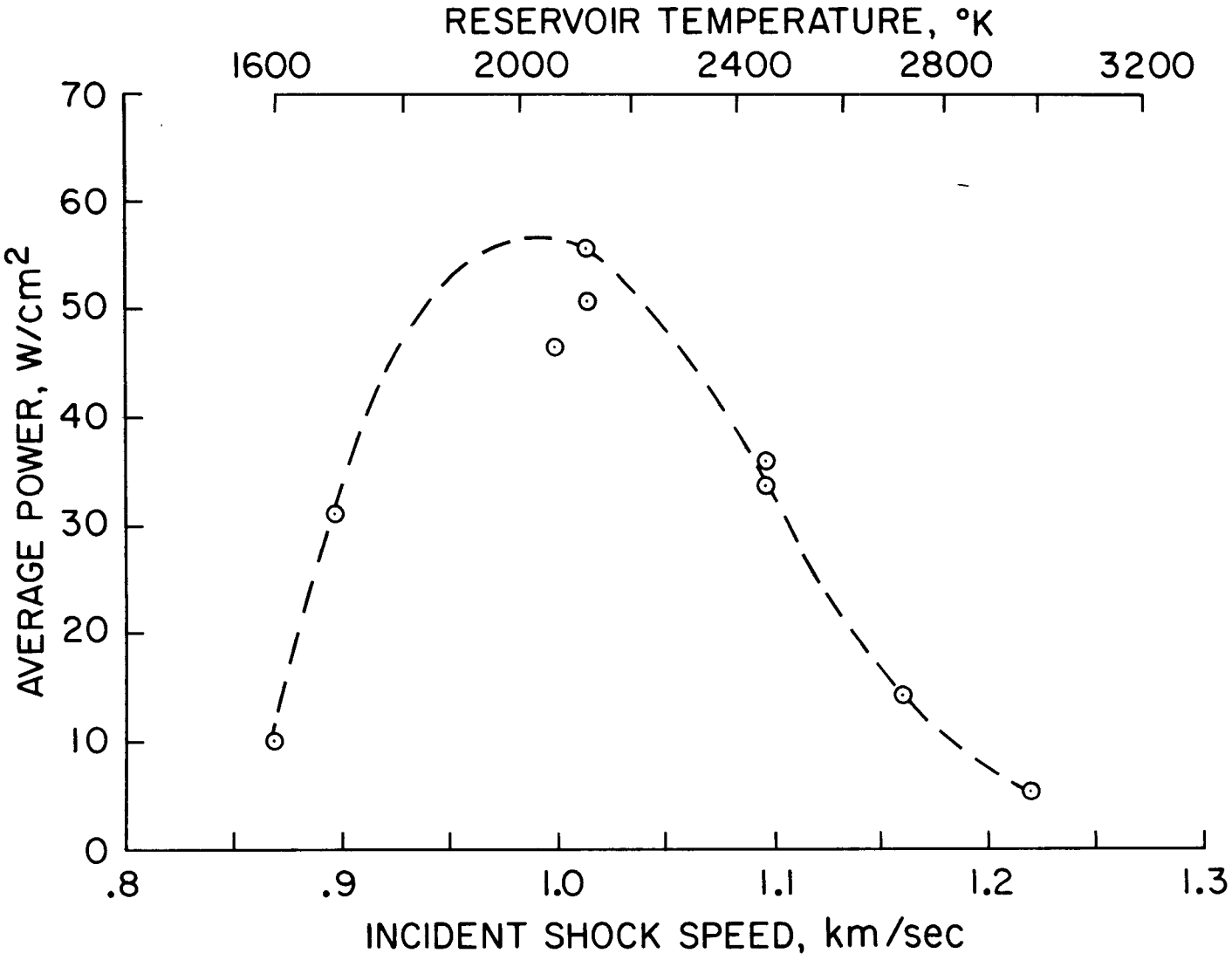
RESERVOIR TEMPERATURE, °K
1600
2000
2400
2800
3200
70
60
50
40
30
20
10
0
AVERAGE POWER, W/cm2
.8
.9
1.0
1.1
1.2
1.3
INCIDENT SHOCK SPEED, km/sec

Figure 12

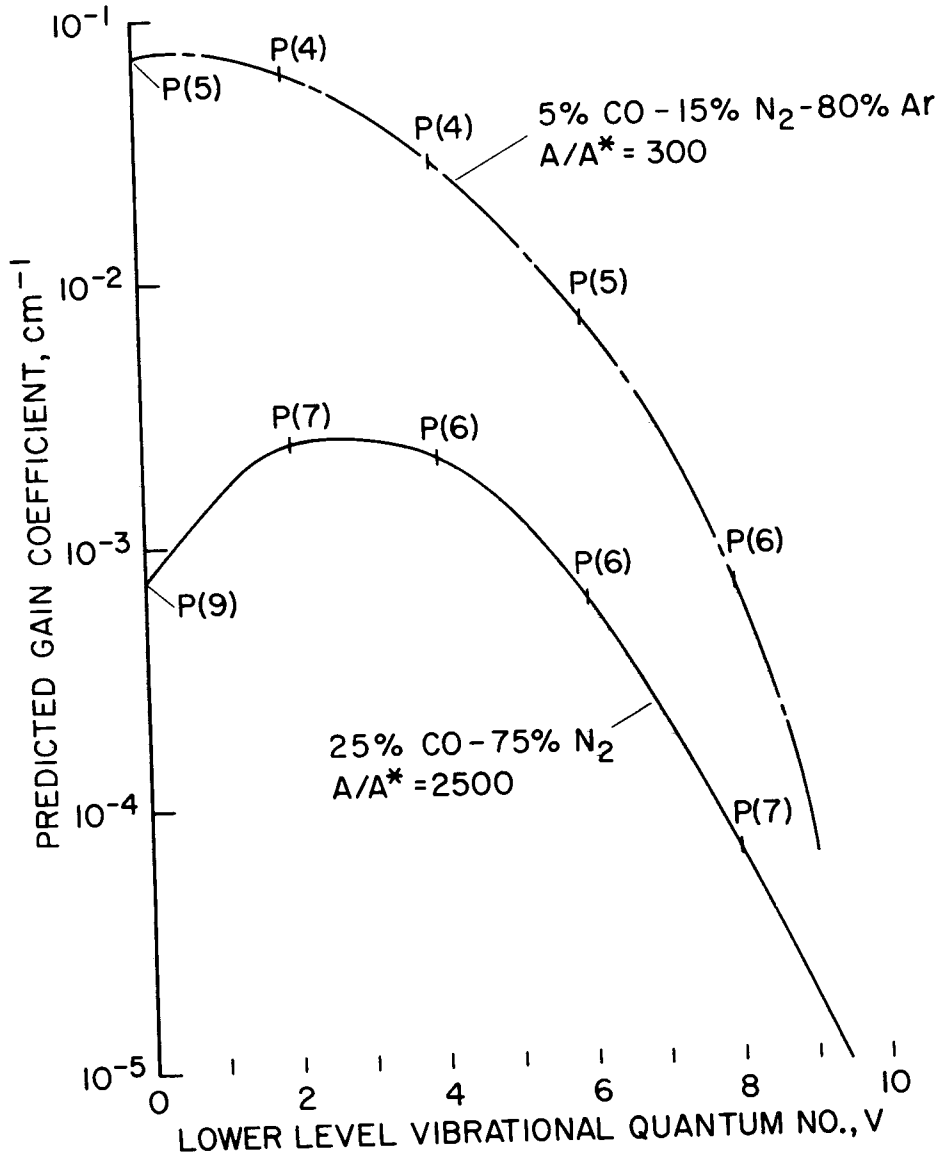
10^{-1}
10^{-2}
10^{-3}
10^{-4}
10^{-5}
PREDICTED GAIN COEFFICIENT, cm^{-1}
P(4)
P(5)
P(4)
5% CO - 15% N_2 - 80% Ar
$A/A^* = 300$
P(5)
P(7)
P(6)
P(6)
P(9)
P(6)
25% CO - 75% N_2
$A/A^* = 2500$
P(7)
0
2
4
6
8
10
LOWER LEVEL VIBRATIONAL QUANTUM NO., V

Figure 13